Theoretical Study of Formic Acid Anhydride Formation from Carbonyl Oxide in the Atmosphere

P. Aplincourt and M. F. Ruiz-López*

Laboratoire de Chimie Théorique, UMR CNRS-UHP No. 7565,† Université Henri Poincaré - Nancy I, B.P. 239, 54506 Vandoeuvre-lès-Nancy Cedex, France

Received: August 10, 1999; In Final Form: November 9, 1999

We report the first theoretical study on the formation mechanism of tropospheric formic acid anhydride (FAA). Experimental studies on this subject have raised controversy, and the reaction mechanisms proposed are examined here with the help of theoretical calculations at the density functional theory and various correlated ab initio levels (MP4, CCSD, CASSCF, CASPT2) using extended basis sets. The investigated processes are initiated by the reaction of carbonyl oxide with either formaldehyde or formic acid. In the first case, a secondary ozonide is formed that then isomerizes to hydroxymethylformate (HMF). Stepwise and concerted mechanisms have previously been proposed for the isomerization process on the basis of experimental results. Our calculations confirm the existence of both mechanisms, but the stepwise one appears to be more favorable. HMF decomposition into FAA and H_2 is shown to be unlikely (activation barrier about 90 kcal/mol). Conversely, reaction of HMF with molecular oxygen in the singlet state leads to FAA and H_2O_2 through a small barrier close to 9 kcal/mol at the B3LYP level. In the case of the carbonyl oxide + formic acid pathway, the transitory product is hydroperoxymethylformate (HPMF). Decomposition of HPMF into FAA and H_2O proceeds through a large activation barrier (about 50 kcal/mol). The process may be assisted by a formic acid molecule, lowering the activation barrier for FAA formation to 29.8 kcal/mol at the B3LYP level. Reactions energies are −113.7 kcal/mol for $H_2COO + H_2CO \rightarrow FAA + H_2$, −174.6 kcal/mol for $H_2COO + H_2CO + O_2 \rightarrow FAA + H_2O_2$, and −101.7 kcal/mol for $H_2COO + HCOOH \rightarrow FAA + H_2O$ (values at the B3LYP level with ZPE corrections). Therefore, the mechanism involving singlet O_2 appears to be the most favorable one in atmospheric conditions, both kinetically and thermodynamically.

1. Introduction

In the urban atmosphere, an important number of chemical processes take place. Pollutant gases, such as hydrocarbons or oxides of nitrogen and sulfur, react to create a variety of products including ozone, which in turn might be involved in a variety of oxidation processes. Among these reactions, that with alkenes, and in particular with ethene, has received much attention in recent years because it plays a major role in urban air pollution phenomena.[1] In addition, it has been shown that the gas-phase ozonolysis of biogenic compounds, as isoprene and terpenes, is a nighttime source of hydroxyl radicals.[2] The main features of ozonolysis have been first described by Criegee[3] and are now relatively well understood. Initially, the alkene double-bond cleavage by ozone leads to a primary ozonide, which rapidly decomposes in carbonyl compounds and carbonyl oxides RR′COO,[4,5] that are produced in vibrationally excited states (see Scheme 1).

Carbonyl oxides can undergo decomposition and isomerization reactions to yield CO, CO_2, H_2O, OH, H_2, HCOOH, or dioxirane[2,6−8] or can be collisionally stabilized and react with carbonyl compounds,[6,9,10] CO,[9] SO_2,[11] or HCOOH,[12] for example. All these processes are summarized in Scheme 2 for H_2COO. The decomposition/stabilization ratio k_1/k_2 is very dependent on the alkene considered and on the total pressure.[11,13] For ozone addition to ethene, about 60% of the H_2COO produced undergoes unimolecular reactions, whereas the other 40% gives rise to bimolecular reactions.[14]

SCHEME 1

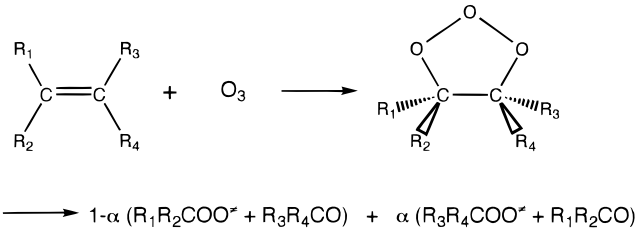

SCHEME 2

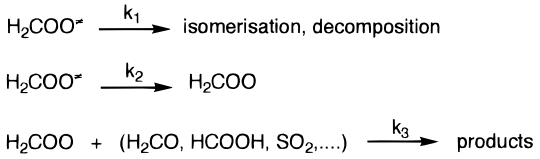

There are many unknown aspects on the gas-phase chemistry of carbonyl oxides. Several mechanisms, rate constants, and products from the above reactions are uncertain. In particular, there is some experimental controversy on the reaction mechanism leading to formic acid anhydride (FAA) formation. This compound was shown to be a major product of the ozonolysis reaction when carried out in atmospheric conditions, typically O_3 (11.8 ppm) and C_2H_4 (9.56 ppm) in O_2 (25 Torr) and N_2 (675 Torr).[9] The influence of adding about 10 ppm of aldehyde

* To whom correspondence should be addressed. Tel: (33) 3 83 91 20 50. Fax: (33) 3 83 91 25 30. E-mail: Manuel.Ruiz@lctn.u-nancy.fr.
† Part of the Institut Nancéien de Chimie Moléculaire.

10.1021/jp9928208 CCC: $19.00
Published on Web 12/21/1999

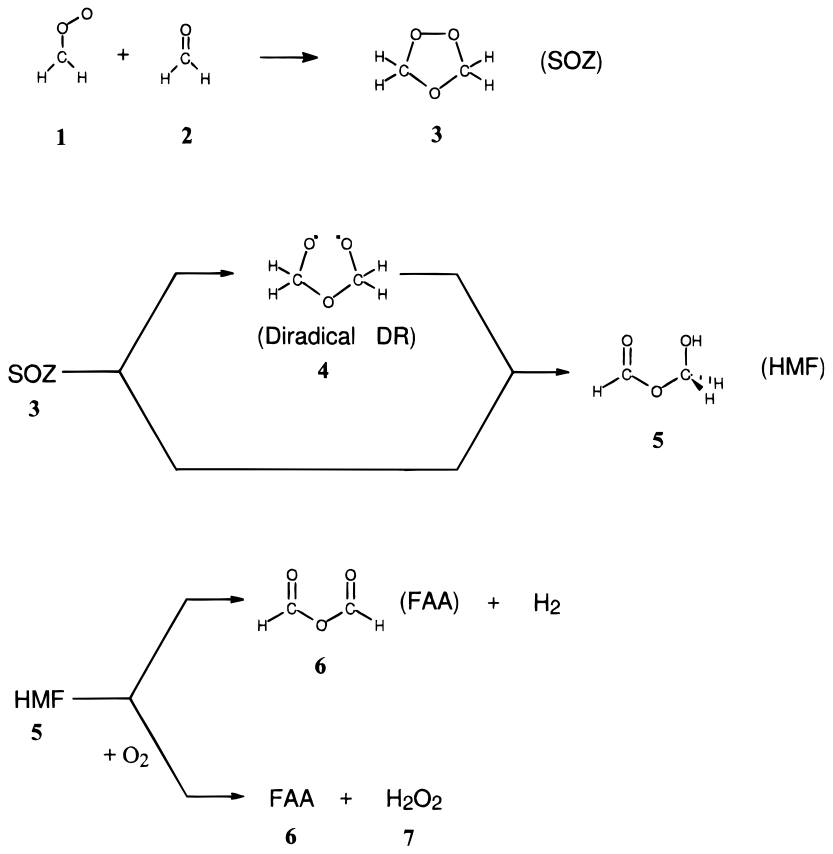

Figure 1. Proposed mechanisms for FAA formation. The initial reaction is $H_2COO + H_2CO$.

(CH_2O or CH_3CHO) to the initial $O_3-C_2H_4$ mixture was also investigated. The authors concluded that carbonyl oxide may survive decomposition and take part in bimolecular reactions involving CH_2O and CH_3CHO as well as other species present in the polluted atmosphere. Other experiments were carried out by Neeb et al.[12] that compared the effect of adding CH_2O (5−30 ppmv) and HCOOH (1−10 ppmv) to the mixture.

On the basis of these laboratory experiments, two main FAA formation mechanisms have been envisaged. The first one starts with the reaction of carbonyl oxide and formaldehyde and was initially studied by Su et al.[9] and later by Hull et al.[15] and Kan et al.[16] The mechanism is represented in Figure 1. Su et al.[9] studied the kinetics and products of the reaction between ozone and ethene by Fourier transform infrared (FTIR) spectroscopy. In addition to the expected products, CO, CO_2, CH_2O, or HCOOH, they observed additional bands on their spectra that were assigned to two other products, FAA and hydroxymethyl formate (HMF). The latter was assumed to be a transitory product for FAA. In the first step, carbonyl oxide **1** and formaldehyde **2** react to form the secondary ozonide **3** (SOZ). Next, this highly reactive ozonide yields HMF **5** through either a two-step mechanism (via a diradical intermediate **4**)[9] or a concerted one.[15] Finally, dehydrogenation of HMF yields FAA **6**. This final step could also proceed by the reaction of HMF with molecular oxygen yielding FAA and H_2O_2 **7**.[16] Note that a photolytic decomposition of HMF has also been reported.[17]

The second main pathway for FAA formation assumes that carbonyl oxide reacts with formic acid **8**. The corresponding mechanism was described by Neeb et al.[12] and is given in Figure 2. On the basis of some thermochemical considerations and on the reaction of **1** with alcohols in the liquid phase,[18] the authors suggested a two-step mechanism in which the transitory product would be hydroperoxymethyl formate **9** (HPMF), which would decompose slowly to FAA and water.

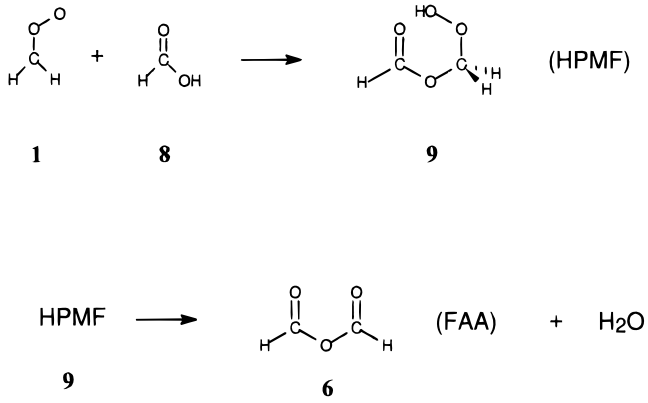

Figure 2. Proposed mechanisms for FAA formation. The initial reaction is $H_2COO + HCOOH$.

Many theoretical works have been devoted to the chemistry of carbonyl oxides from the first ab initio calculation of Ha et al.[19] 25 years ago (see, for instance, refs 2 and 19−34). They have focused on unimolecular processes, mainly isomerization to dioxirane, reactions with carbonyl compounds to yield SOZs, oxygen-transfer reactions, etc. However, the mechanisms that lead to FAA in the atmosphere have not been theoretically investigated, in contrast with the interest that they have raised experimentally. In this work, we study those reactions that have previously been invoked to explain FAA formation.[9,10,12,15,16] One should note that the concentrations of the compounds in the troposphere may vary considerably, and therefore, the relative importance of the reactions needs to be considered. Our work focuses on the description of transition states and reaction energetics. Theoretical computations have been carried out to explore the potential energy surfaces, locate transition structures, and evaluate activation barriers and reaction energies. Different

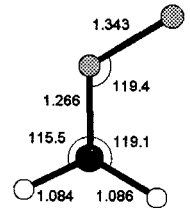

Carbonyl Oxide

1

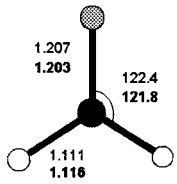

Formaldehyde

2

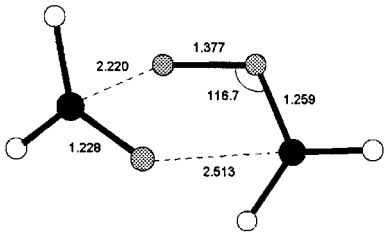

1-2 Complex

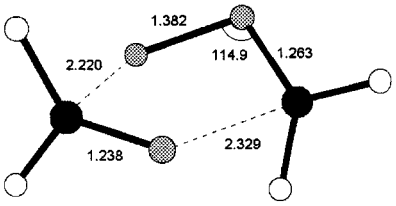

TSa

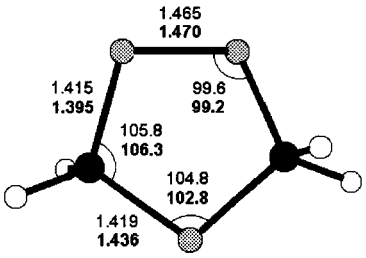

Secondary Ozonide (SOZ)

3

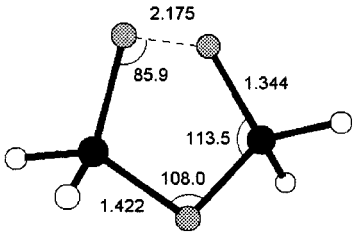

TSb

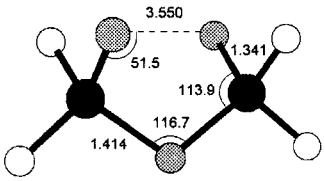

Diradical (DR)

4

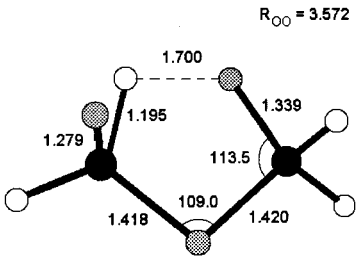

TSc

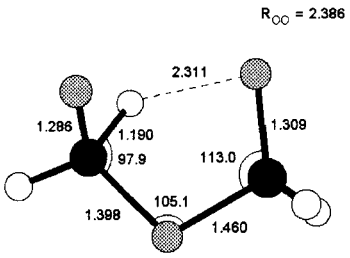

TSd

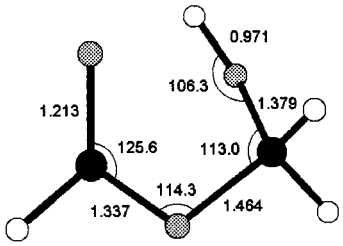

Hydroxymethyl formate

(HMF cis)

5

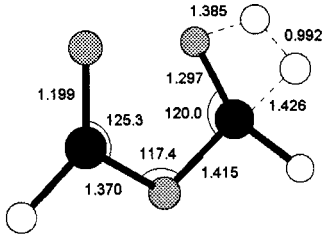

TSe

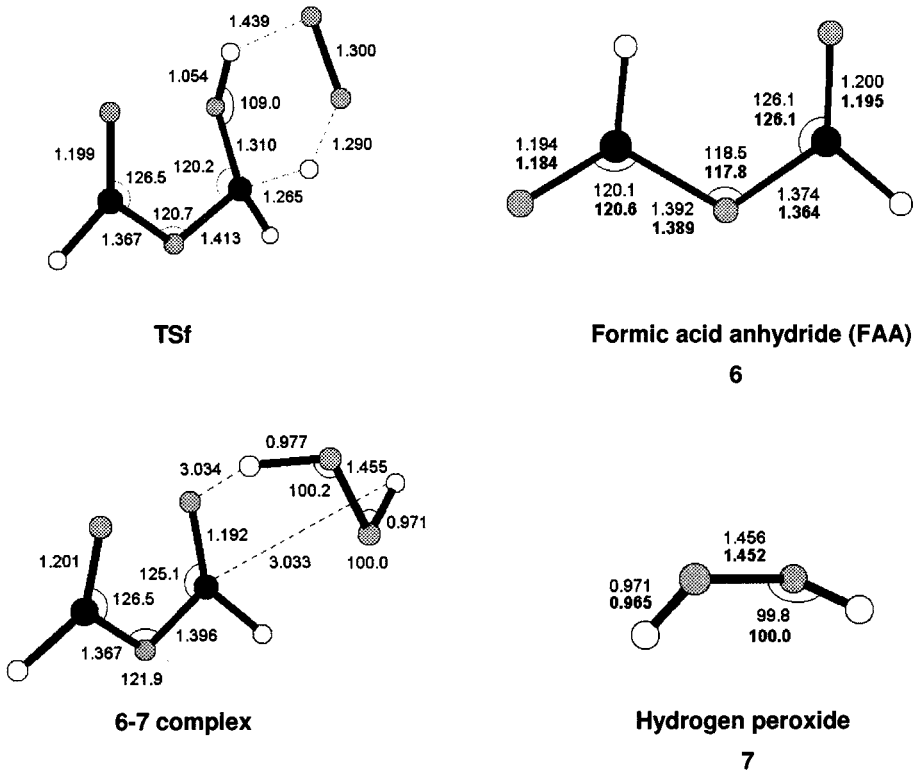

Figure 3. B3LYP/6-31G(d,p)-computed structures for species in the FAA formation mechanisms initiated by the reaction $H_2COO + H_2CO$. Values are in angstroms and degrees. Available experimental values are in bold. C, O, and H atoms are drawn in black, gray, and white, respectively.

theoretical approaches have been used including density funtional methods and high-level correlated ab initio techniques.

2. Computational Method

To get a good compromise between accuracy and computational cost, the methodological level has been chosen on the basis of conclusions reached in previous studies for related systems. For instance, Gutbrod et al.[30] have demonstrated that density functional calculations at the B3LYP/6-31G(d,p) level reproduce the geometrical parameters of carbonyl oxide obtained by CCSDT(T)/TZ+2P calculations[7] and have used this method to optimize the structures of interest, in particular, transition states with H-atom transfers close to those encountered in our work (see ref 35 for technical details and references on theoretical methods and basis sets cited in this paper). Accordingly, the structures studied here have been optimized at the B3LYP/6-31G(d,p) level. Afterward, using such geometries, single-point energy calculations have been made at the B3LYP, MP4(SDTQ), and CCSD(T) levels with the 6-311G(d,p) basis set.

The case of diradical species has received a specific treatment and requires further comments. On one hand, the value of $\langle S^2 \rangle$ corresponding to the Hartree−Fock wave function indicated that the singlet electronic state was strongly contaminated by the first triplet state (computed value being 0.7−1.0 instead of 0.0). This feature may lead to unrealistic energies, and following previous works,[36] we have decided to correct spin contamination effects in MP4 results by annihilating the largest spin contaminant (projected MP4 or PMP4 method).[37] Previous studies have shown that this correction leads to a much better agreement between experimental and theoretical barrier heights.[38] On the other hand, CASSCF and CASPT2 have been used to evaluate the barrier heights in this case, since these approaches, which allow us to define pure spin configurations, are suited to treat diradical species. The active space has been adjusted to each individual reaction step since the chemical bonds involved change and a general scheme was not possible. For the reaction SOZ **3** → diradical **4**, we have considered six electrons and six active molecular orbitals corresponding to the OO and CO bonding and antibonding orbitals (CASSCF(6,6)). For the diradical **4** → HMF **5** process, the choice has been four electrons and four active molecular orbitals corresponding to the OO and CH bonding and antibonding orbitals (CASSCF(4,4)). CASSCF and CASPT2 calculations have been carried out using the ANO basis set (contractions are (10s6p3d/3s2p1d) for C and O and (7s3p/2s1p) for H).

For all the transition structures (TSs), we have verified that the Hessian matrix leads to only one imaginary frequency, and we have carried out intrinsic reaction coordinate (IRC) calculations[39] in order to identify the species connected by a particular TS. Zero-point energy (ZPE) was calculated by scaling analytical harmonic B3LYP/6-31G(d,p) frequencies by 0.963 [40]. All the calculations have been carried out with Gaussian 94 [41] and MOLCAS programs,[42] the latter being used for the multiconfiguration approach calculations.

For simplicity, in the discussion below we use B3LYP values with ZPE corrections (unless otherwise stated) because they are available for all the reaction steps. In general, all the methods predict the same trends. When significant differences are found in a particular case, it is commented in the text.

3. Study of the $H_2COO + H_2CO$ Reaction

We first analyze the mechanism depicted in Figure 1, first proposed by Su et al.[9] and later by Hull et al.[15] and Kan et al.[16] The presentation of the results is separated in the following reaction steps: (1) formation of SOZ, (2) formation of the transitory product HMF, and (3) formation of FAA. The B3LYP/6-31G(d,p)-optimized geometries for all the species of interest are collected in Figure 3. Experimental values are given when

TABLE 1: Relative Energies (in kcal/mol) for the Reaction of Carbonyl Oxide with Formaldehyde[a]

	B3LYP	MP4 (SDTQ)	CCSD (T)	ZPE
SOZ Formation				
H_2COO (**1**) + H2CO (**2**)	0.0	0.0	0.0	0.0
1−**2** complex	−8.8	−8.2	−7.5	+1.7
TSa	−8.4	−7.7	−6.7	+2.1
SOZ (**3**)	−51.8	−56.9	−55.0	+6.0
HMF Formation				
stepwise process				
SOZ (**3**)	0.0	0.0	0.0	0.0
TSb	21.9	20.8 (36.1)		−3.4
DR (**4**)	17.8	15.0 (28.4)		−4.0
TSc	24.7	25.8 (45.5)		−6.1
HMF (**5**)	−78.3	−80.1	−78.6	+0.1
concerted process				
TSd	48.1	33.6	40.4	−4.2
FAA Formation				
dehydrogenation				
HMF (**5**)	0.0	0.0	0.0	0.0
TSe	93.1	95.6	97.3	−6.4
FAA (**6**) + H_2	19.4	18.6	20.2	−9.1
reaction with O_2				
HMF (**5**) + $O_2(^1\Delta_g)$	0.0	0.0	0.0	0.0
TSf	11.8	20.9	25.9	−3.2
6−**7** complex	−54.2	−46.7	−46.3	−0.2
FAA (**6**) + H_2O_2 (**7**)	−49.1	−40.7	−40.7	−1.5

[a] The geometries have been optimized at the B3LYP/6-31G(d,p) level. Energies are computed using those geometries and the 6-311G(d,p) basis set with the methods indicated. ZPE corrections are obtained using the B3LYP/6-31G(d,p) computed frequencies scaled by 0.963. The energies are relative to the total energy of initial reactants for each reaction step. MP4 values for HMF formation have been computed using the projected MP4 method (unrestricted-MP4 values are given in parentheses for comparison).

available. In Table 1, we give the relative energies and ZPE corrections for all the reaction steps considered.

3.1. Formation of SOZ. Geometrical parameters for SOZ **3** are given in Figure 3 and are in good agreement with experimental data.[43]

On the basis of MP4 results, Cremer[26] has suggested that formation of SOZ from H_2COO and H_2CO proceeds through the formation of a van der Waals complex that lies in a very flat potential energy surface and displays a very low activation energy toward SOZ formation. The existence of such an energy minimum depends substantially on computational level. In particular, it is not found at the B3LYP/6-31G(d,p) level but exists at the B3LYP/6-31+G(d,p) level.[44] Since such a structure does not play a fundamental role in our context (see below), we have simply employed previously reported geometries.[44]

Inspection of energy values in Table 1 for this reaction step reveals a good agreement between results obtained at different levels. The complexation energies compare well with the MP4-(SDQ)/6-31G(d,p) calculation performed by Cremer et al. (−8.9 kcal/mol without ZPE).[14] The activation energy to form the secondary ozonide **3** is 0.8 kcal/mol, confirming the small magnitude of the activation barrier. This is explained by the close similarity between the complex and TS geometries, as shown in Figure 3. The reaction is characterized by a substantial exothermicity ($\Delta E_{B3LYP} + \Delta ZPE = -45.8$ kcal/mol).

3.2. Formation of the Transitory Product (HMF). Kinetic and spectroscopic characterizations of HMF **5** were made by Niki et al.[10] The authors have interpreted the results obtained in their residual spectra by the occurrence of an equilibrium between two isomers of **5**, trans and cis. In addition to these conformations, we have found an intermediate gauche structure. Our calculations give the cis form as the most stable isomer whatever the method used. For instance, at the B3LYP level and taking into account ZPE, the trans and gauche structures are 2.9 and 2.4 kcal/mol above the cis conformation, respectively. This may be understood by the presence of an intramolecular OH hydrogen bond in the cis conformer. Only the HMF cis geometry is drawn in Figure 3.

TABLE 2: Relative Energies (in kcal/mol) Calculated for the Formation of Transitory Product (HMF) from Secondary Ozonide by a Stepwise Mechanism[a]

	CASSCF		CASPT2	
	(6,6)	(4,4)	(6,6)	(4,4)
stepwise process				
SOZ (**3**)	0.0		0.0	
TSb	26.9		22.3	
DR (**4**)	23.5	0.0	21.2	0.0
TSc		7.7		9.4

[a] Energy calculations at the CASSCF and CASPT2 levels with ANO basis sets over optimized geometries at the B3LYP/6-31G(d,p) level.

As shown in Figure 1, two different ways have been considered to explain the decomposition reaction SOZ **3** → HMF **5**. The first one is a two-step mechanism proceeding through the formation of an intermediate diradical **4**.[9] The second one is a concerted mechanism in which OO bond cleavage and hydrogen transfer are simultaneous.[15]

Stepwise Process. The homolytic cleavage of the OO bond in **3** is accompanied by a small shortening of the two CO bond types (cf. Figure 3). The transition structure already displays a strong diradical character with spin-densities concentrated on oxygen atoms (B3LYP values being ±0.701). Obviously, this trend is enhanced in the diradical **4** (±0.866). Afterward, **4** isomerizes to HMF **5** by H-atom transfer, so that the process is accompanied by a loss of the C_2 molecular symmetry. The geometry of the corresponding transition structure **TSc** is close to that of the diradical, and accordingly, oxygen atoms spin-densities are still large (+0.590 and −0.643).

As previously described, projected-MP4 and multiconfigurational CAS energy calculations have been carried out in this case (see the computational section for details). CASSCF and CASPT2 results are presented in Table 2. Looking at the energies in Tables 1 and 2, the following remarks might be made. The differences between projected-MP4 and unrestricted-MP4 results are substantial, as expected on the basis of strong Hartree−Fock spin contamination. Independently of the computational level, the diradical formation is clearly more difficult (activation energy being 18.9 kcal/mol at the CASPT2 level with ZPE) than HMF formation from the diradical (7.3 kcal/mol with the same method). The predicted energy difference between the highest TS (**TSc**) and SOZ is consistent with experimental activation energy measurements (27.5 ± 1.5 kcal/mol).[15]

Activation energies for the diradical formation may be compared to other OO bond homolytic cleavage in related systems. Indeed, the activation energy for reaction **3** → **4** is substantially lower than the one found experimentally for simple peroxides[45,46] such as diethyl peroxide (31.7 kcal/mol), dipropyl peroxide (35 kcal/mol), or hydrogen peroxide (54 kcal/mol). Note that B3LYP calculations for H_2O_2 and $(CH_3CH_2)_2O_2$ dissociation energies are in good agreement with experiment, predicted values being 54.1 and 36.3 kcal/mol, respectively.

Concerted Process. B3LYP calculations led to transition structure **TSd** in Figure 3. The energy of this TS is much higher than that computed for the stepwise transition structures. The activation energy is therefore substantial (43.9 kcal/mol), and a concerted isomerization of SOZ to HMF is not likely to occur.

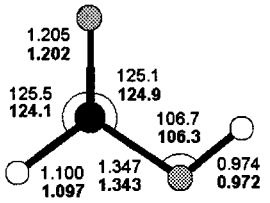

Formic acid

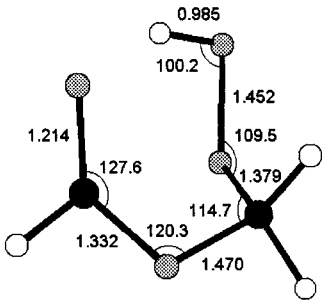

Hydroperoxymethyl formate (HPMF cis) 9

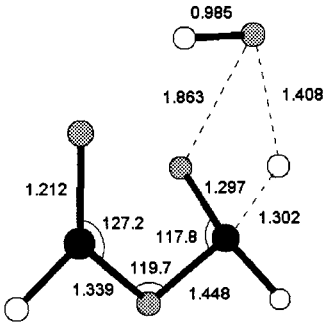

TSg

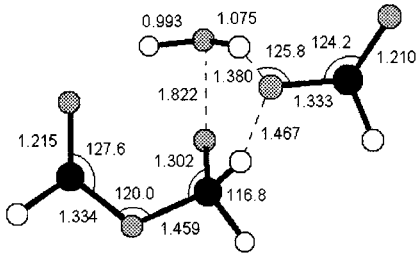

TSh

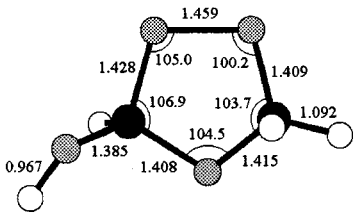

HSOZ

Figure 4. B3LYP/6-31G(d,p)-computed structures for species in the FAA formation mechanisms initiated by the reaction H_2COO + HCOOH. Values are in angstroms and degrees. Available experimental values are in bold. C, O, and H atoms are drawn in black, gray, and white, respectively.

Notice, however, that in this case the difference between B3LYP and MP4 calculations is noticeable so that more accurate results would require to perform geometry optimizations at higher levels.

3.3. Formation of FAA. Before discussing HMF decomposition mechanisms, let us make a few comments on the structure of the final product, FAA. Electron diffraction and microwave spectroscopic studies led to the conclusion that the most stable conformation of FAA in the gas phase is the synperiplanar, antiplanar [sp,ap] one (defined by the two torsion angles O═C−O−C) at room temperature.[47] Our results confirm this result since the two others conformers, [sp,sp] and [ap,ap], lie, respectively, 2.8 and 3.3 kcal/mol above the [sp,ap] one at the B3LYP level. Only the structure of the most stable conformer is given in Figure 3. Comparison with experimental data reveals that the B3LYP method correctly predicts geometry parameters. In addition, we have computed the rotation barrier connecting the C_s [sp,ap] and the C_{2v} [sp,sp]. The B3LYP value (5.2 kcal/mol) is not far from the barrier measured by dynamic NMR in solution (4.3 kcal/mol[48]). Note that the effect of the environment is expected to lower the activation barrier since the dipole moment increases from the [sp,ap] to the [sp,sp] conformation.

Previous work[9] suggested that decomposition of HMF requires the passage through a four-membered-ring transition state, yielding FAA **6** and H_2. We have succeeded in locating such a transition structure (**TSe**, see Figure 3), but the corresponding activation energy (see Table 1) is extremely high (not far from 90 kcal/mol), and therefore, this first-order process is very unlikely to take place under atmospheric conditions.

Kan and co-workers[16] have hypothesized that FAA is formed from the reaction between HMF and molecular O_2, which also yields H_2O_2. In principle, both singlet and triplet molecular

TABLE 3: Relative Energies (in kcal/mol) for the Reaction of Carbonyl Oxide with Formic Acid[a]

	B3LYP	MP4 (SDTQ)	CCSD (T)	ZPE
HPMF Formation				
H_2COO (**1**) + HCOOH (**8**)	0.0	0.0	0.0	0.0
HPMF (**9**)	−45.7	−50.4	−47.8	+3.7
FAA Formation				
unimolecular process				
HPMF (**9**)	0.0	0.0	0.0	0.0
TSg	53.8	50.4	53.1	−4.8
FAA (**6**) + H_2O	−55.5	−60.0	−58.6	−4.2
assisted process				
HPMF (**9**) + HCOOH (**7**)	0.0	0.0		0.0
TSh	33.9	39.6		−4.1
FAA (**6**) + H_2O + HCOOH (**8**)	−55.5	−60.0		−4.2

[a] The geometries have been optimized at the B3LYP/6-31G(d,p) level. Energies are computed using those geometries and the 6-311G(d,p) basis set with the methods indicated. ZPE corrections are obtained using the B3LYP/6-31G(d,p) computed frequencies scaled by 0.963. The energies are relative to the total energy of initial reactants for each reaction step.

oxygen may react with HMF. Indeed, singlet O_2 is at a relatively high concentration in the troposphere. It is mainly generated by the photolysis of ozone and contrary to the $O(^1D)$ atom, and it is quenched only slowly at atmospheric pressure. The singlet−triplet energy difference is large, about 23 kcal/mol,[49] so that one may expect the singlet state to be more reactive than the fundamental triplet state. Taking into account these remarks, we have decided to investigate the FAA + O_2 ($a^1\Delta_g$) reaction only. The reaction with triplet O_2 can also be envisaged, but it is computationally much more complex and would deserve a separate study.

The reaction of **5** with singlet O_2 is predicted to proceed via a six-center transition state **TSf** drawn in Figure 3. The activation barrier found, 8.6 kcal/mol (see Table 1), is indeed much lower than the one computed for the process **5** → FAA + H_2. The products, FAA and H_2O_2, form a complex which is 3.8 kcal/mol more stable than the separated compounds. The predicted reaction energy is substantial (−50.6 kcal/mol) and comparable to that found for SOZ formation. Taking into account the singlet−triplet energy difference for O_2 (23 kcal/mol[49]), the computed reaction energy is consistent with the experimental data of Kan et al.[16] ($\Delta H \cong -14$ kcal/mol).

4. Study of the H_2COO + HCOOH Reaction

We consider now the mechanism depicted in Figure 2, proposed by Neeb et al.[12] The results are presented by considering the following steps: (1) formation of the transitory product HPMF and (2) formation of FAA. The B3LYP/6-31G-(d,p)-optimized geometries for all the species of interest are collected in Figure 4. Experimental values are given when available. Energies are gathered in Table 3. As before, we give the relative and zero-point energies (ZPEs) for the reaction steps considered.

4.1. Formation of the Transitory Product, HPMF. In principle, the carbonyl oxide + formic acid reaction may proceed in two different modes. On one hand, carbonyl oxide may attack the OH group, similarly to reaction with alcohols,[18] yielding hydroperoxymethyl formate HPMF **9** (see Figure 4). On the other hand, carbonyl oxide may attack the CO double bond, similarly to the reaction with aldehydes (see above), yielding a hydroxylated ozonide HSOZ (see Figure 4). In both cases, the adduct formation appears to be barrierless. Indeed, no transition state or stable complex could be located in our study despite a detailed analysis of the potential energy surface. Moreover, geometry optimizations with different starting points systematically led to the adduct. Therefore, exothermicity should be an essential factor. The reaction energies for HPMF and HSOZ formation are −42.0 and −27.5 kcal/mol, respectively. Thus, our computations indicate that HPMF is substantially more stable than the hydroxylated ozonide by 14.5 kcal/mol. Accordingly, HPMF should be the transitory product, as suggested by Neeb and co-workers.[12]

SCHEME 3

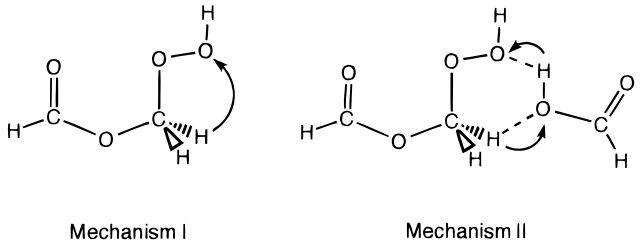

HPMF, like HMF, exhibits three different conformations cis, trans, and gauche, the former being the most stable one. The larger stability of the cis conformer is explained by the presence of an intramolecular O−H hydrogen bond, clearly seen in Figure 4 and confirmed by spectroscopic measurements.[12] The trans and gauche conformations lie 2.0 and 4.2 kcal/mol above the cis one, respectively (B3LYP level with ZPE).

4.2. Formation of FAA. The reaction mechanism for HPMF decomposition is unknown. We have postulated here two different pathways shown in Scheme 3: Mechanism I involves an intramolecular H-transfer, whereas mechanism II corresponds to a bimolecular reaction in which H-transfer is promoted by an ancillary formic acid molecule.

Transition structures for both mechanisms have been located and are described in Figure 4. Computed energies in Table 3 show that the activation energy for reaction mechanism I is substantially larger than for mechanism II (49.0 vs 29.8 kcal/mol).

The computed value for the HPMF → FAA + H_2O reaction energy (−59.7 kcal/mol) is in very good agreement with thermochemical data (−56.2 kcal/mol[12]). Note that the reaction is more exothermic than the reaction of HMF with singlet molecular oxygen to yield FAA and H_2O_2 (−50.6 kcal/mol). Note that this trend is more marked at the MP4 and CCSD levels because the predicted exothermicities for the HPMF → FAA + H_2O reaction are larger whereas those for the HMF + O_2 → FAA + H_2O_2 are smaller.

5. Discussion

Let us now compare all the processes described above. We focus our discussion on the reaction energetics but one should keep in mind that the actual reaction kinetics in the atmosphere depends on the initial concentrations of the reactants. These data may vary importantly in polluted atmosphere or laboratory experiment conditions. As before, we mainly use B3LYP values for comparison purposes but the trends are reproduced by all the methods.

Carbonyl oxide reacts exothermically with formaldehyde and formic acid. If both substances are present, the reaction with formaldehyde is slightly preferred thermodinamically. Indeed, the formation energy for the transitory product HPMF (−42.0 kcal/mol) is slightly smaller than that for SOZ formation (−45.8 kcal/mol). Moreover, both HPMF and SOZ are formed without significant activation barriers. The decomposition of these

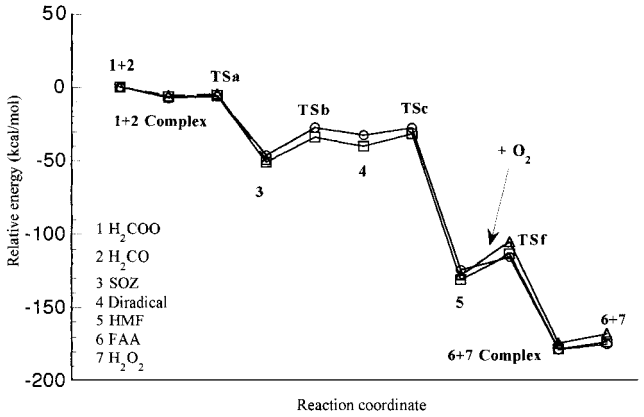

Figure 5. Comparison of energy profiles for the most favorable FAA formation mechanism. Energies were obtained at the B3LYP (circles), MP4 (squares), and CCSD (triangles) levels using the 6-311G(d,p) basis set and the B3LYP/6-31G(d,p) optimized geometries.Values include ZPE corrections at the B3LYP/6-31G(d,p) level. For **TSb**, **4**, and **TSc**, MP4 relative energies correspond to results using the projected-MP4 method. For those structures, no CCSD values were computed (see Table 2 for CASSCF and CASPT2 values).

intermediate species yields FAA and always involves an activation barrier.

A comparison of the predicted energy profiles for the most favorable reaction mechanism is presented in Figure 5. As noted, all the methods lead to similar conclusions although the absolute quantities may change a little. The whole reaction energies for the relevant processes are:

$$H_2COO + H_2CO \rightarrow FAA + H_2 \qquad \Delta E = -113.7 \text{ kcal/mol} \quad (1)$$

$$H_2COO + H_2CO + O_2 \rightarrow FAA + H_2O_2 \qquad \Delta E = -174.6 \text{ kcal/mol} \quad (2)$$

$$H_2COO + HCOOH \rightarrow FAA + H_2O \qquad \Delta E = -101.7 \text{ kcal/mol} \quad (3)$$

This comparison shows that reactions 1 and 3 are substantially less exothermic than 2 by about 60−70 kcal/mol. Reaction 1 is more exothermic than 3 by a little more than 10 kcal/mol. Examination of the activation barriers shows that reaction 2 is kinetically more favorable than either 1 or 3. The rate-limiting step of such a mechanism is the isomerization of SOZ into HMF. The activation energy required (18.6 kcal/mol for the relative energy of **TSc** with respect to SOZ) is significantly below the value for the decomposition of HPMF (29.8 kcal/mol).

6. Conclusion

All the methods employed in this work lead to the same qualitative conclusions. In most cases, they give close results so that the B3LYP approach appears to be a good compromise between computational cost and accuracy. This is an interesting result that should be useful in future applications to investigate the reactions of substituted carbonyl oxides.

Though the mechanism of FAA formation from carbonyl oxide in the atmosphere appears to be rather complex, our computations allow us to elucidate a few points. First, the original mechanism of Su et al. is very unlikely since the decomposition of HMF into FAA and H_2 requires a very large activation energy. Second, carbonyl oxide reacts spontaneously with formadehyde or formic acid but the exothermicity is larger in the first case. Besides, our results predict that the reaction with formic acid proceeds through attack to the OH group rather than to the CO group. Another interesting result is that the homolytic breaking of the OO bond in the secondary ozonide is much easier than in the case of open peroxides, so that isomerization of the ozonide into the transitory product HMF is less difficult than expected. Moreover, isomerization through a concerted process appears to be unlikely.

According to our computations, if molecular oxygen is available, in particular in singlet electronic states, the most efficient way for FAA formation would be the reaction of carbonyl oxide with formaldehyde followed by the reaction of the corresponding transitory product HMF with O_2. Analysis of both, reaction and activation energies, supports this conclusion. Nonetheless, the reaction of carbonyl oxide with formic acid yields a transitory product HPMF that may decompose to FAA and water. A striking result is that the latter process can be assisted by a bifunctional molecule that is able to accept and give a proton simultaneously. We have considered the case of an ancillary formic acid molecule, but other compounds, such as water, could also be invoked.

In conclusion, both HMF and HPMF are expected to play a role in the gas-phase ozonolysis reaction. Direct formation of FAA from those intermediates is, however, unlikely. Reaction with another molecule, for instance, O_2 in the case of HMF and HCOOH in the case of HPMF, appears to be a prerequisite. Therefore, the reaction kinetics is expected to change with the experimental conditions, although in the troposphere the reaction of HMF with molecular oxygen is probably the leading mechanism.

References and Notes

(1) Chameides, W. L.; Fehsenfeld, F.; Rodgers, M. O.; Cardelino, C.; Martinez, J.; Parrish, D.; Lonneman, W.; Lawson, D. R.; Rasmussen, R. A.; Zimmerman, P.; Greenberg, J.; Middleton P.; Wang, T. *J. Geophys. Res*. **1992**, *97*, 6037.

(2) Gutbrod, R.; Kraka, E.; Schindler R. N.; Cremer, D. *J. Am. Chem. Soc*. **1997**, *119*, 732. Olzmann, M.; Kraka, E.; Cremer, D.; Gutbrod, R.; Andersson, S. *J. Phys. Chem. A* **1997**, *101*, 9421.

(3) Criegee, R. *Angew. Chem., Int. Ed. Engl.* **1975**, *14*, 745.

(4) Grosjean, E.; Bittencourt de Andrade, J.; Grosjean, D. *Environ. Sci. Technol.* **1996**, *30*, 975.

(5) Grosjean, E.; Grosjean, D. *Environ. Sci. Technol*. **1997**, *31*, 2421.

(6) Horie, O.; Moortgat, G. K. *Atmos. Environm*. **1991**, *25A*, 1881.

(7) Cremer, D.; Gauss, J.; Kraka, E.; Stanton J. F.; Bartlett, R. J. *Chem. Phys. Lett.* **1993**, *209*, 547.

(8) Atkinson R.; Aschmann, S. M. *Environ. Sci. Technol.* **1993**, *27*, 1357.

(9) Su, F.; Calvert, J. G.; Shaw, J. H. *J. Phys. Chem*. **1980**, *84*, 239.

(10) Niki, H.; Maker, P. D.; Savage, C. M.; Breitenbach, P. L. *J. Phys. Chem*. **1981**, *85*, 1024.

(11) Hatakeyama, S.; Kobayashi, H.; Lin, Z.-Y.; Takagi, H.; Akimoto, H. *J. Phys. Chem*. **1986**, *90*, 4131.

(12) Neeb, P.; Horie, O.; Moortgat, G. K. *Chem. Phys. Lett*. **1995**, *246*, 150.

(13) Hatakeyama, S.; Kobayashi, H.; Akimoto, H. *J. Phys. Chem*. **1984**, *88*, 4736.

(14) Atkinson, R.; Lloyd, A. *J. Phys. Chem. Ref. Data* **1984**, *13*, 315. See also ref 6 and references therein.

(15) Hull, L. A.; Hisatsune, I. C.; Heicklen, J. *J. Phys. Chem*. **1972**, *76*, 2659.

(16) Kan, C. S.; Su, F.; Calvert, J. G.; Shaw, J. H. *J. Phys. Chem*. **1981**, *85*, 2359.

(17) Hawkins, M.; Kohlmiller, C. K.; Andrews, L. *J. Phys. Chem*. **1982**, *86*, 3154.

(18) Criegee, R. *Angew. Chem*. **1975**, *87*, 765.

(19) Ha, T. K.; Kühne, H.; Vaccani S.; Günthard H. H. *Chem. Phys. Lett*. **1974**, *24*, 172.

(20) Wadt, W. R.; Goddard, W. A., III. *J. Am. Chem. Soc.* **1975**, *97*, 3004.

(21) Harding L. B.; Goddard, W. A., III. *J. Am. Chem. Soc*. **1977**, *100*, 7180.

(22) Hull, L. A. *J. Org. Chem*. **1977**, *43*, 2780.

(23) Cremer, D. *J. Am. Chem. Soc*. **1979**, *101*, 7199.

(24) Cremer, D. *J. Am. Chem. Soc*. **1981**, *103*, 3627.

(25) Karlström G.; Roos, B. O. *Chem. Phys. Lett.* **1981**, *79*, 416.

(26) Cremer, D.; Kraka, E.; McKee, M. L.; Radhakrishnan, T. P. *Chem. Phys. Lett.* **1991**, 187, 491.

(27) Bach, R. D.; Andrés, J. L.; Owensby, A. L.; Schlegel, H. B.; McDouall, J. J. W. *J. Am. Chem. Soc.* **1992**, *114*, 7207.

(28) Cremer, D.; Gauss, J.; Kraka, E.; Stanton, J. F.; Bartlett, R. J. *Chem. Phys. Lett.* **1993**, *209*, 547.

(29) Anglada, J. M.; Bofill, J. M.; Olivella, S.; Sole, A. *J. Am. Chem. Soc.* **1996**, *118*, 4636.

(30) Gutbrod, R.; Schindler, R. N.; Kraka, E.; Cremer, D. *Chem. Phys. Lett*. **1996**, *252*, 221.

(31) del Rio, E.; Aplincourt, P.; Ruiz-López, M. F. *Chem. Phys. Lett*. **1997**, *280*, 444.

(32) Selçuki, C.; Aviyente, V. *Chem. Phys. Lett.* **1998**, *288*, 669.

(33) Anglada, J. M.; Bofill, J. M.; Olivella, S.; Solé, A. *J. Phys. Chem. A* **1998**, *102*, 3398.

(34) Baboul, A. G.; Schlegel, H. B.; Glukhovtsev, M. N.; Bach, R. D. *J. Comput. Chem.* **1998**, *19*, 1353.

(35) Density Functional calculations are carried out using the hybrid B3LYP functional that combines the three-parameter B3 exchange functional (Becke, A. D. *J. Chem. Phys*. **1993**, *98*, 5648) and the LYP correlation functional (Lee, C.; Yang, W.; Parr, R. G. *Phys. Rev. B* **1988**, *37*, 785). For Möller−Plesset (MP2, MP4) and coupled cluster (CC) methods, see, for instance: Szabo, A.; Ostlund, N. S. *Modern Quantum Chemistry: Introduction to Advanced Electronic Structure Theory*; Macmillan: New York, 1986. For multiconfiguration SCF methods (MCSCF), see, for instance: Roos, B. O. *Ab initio Methods in Quantum Chemistry II*; Wiley: New York, 1987 (for CASSCF) and Roos, B. O.; Anderson, K.; Fülscher, M. P.; Malmqvist, P.; Serrano-Andrés, L.; Pierloot, K.; Merchan, M. *Advances in Chemical Physics, Vol. XCIII*; Wiley and Sons: New York, 1996 (for CASPT2). The references for the basis sets cited in this work are: Hehre, W. J.; Ditchfield, R.; Pople, J. A. *J. Chem. Phys*. **1972**, *56*, 2257 (for 6-31G) and Krishnan, R.; Binkley, J. S.; Seeger, R.; Pople, J. A. *J. Chem. Phys.* **1980**, *72*, 650 (for 6-311G). The usual (d,p) notation holds for polarization orbitals, as proposed in: Hariharan, P. C.; Pople, J. A. *Theor. Chim. Acta* **1973**, *28*, 213. The ANO basis sets are described in: Almlöf, J.; Faegri, K., Jr.; Korsell, K. *J. Chem. Phys.* **1986**, *86*, 4070.

(36) Sosa, C.; Schlegel, H. B. *J. Am. Chem. Soc*. **1987**, *109*, 4193. Sosa, C.; Schlegel, H. B. *J. Am. Chem. Soc*. **1987**, *109*, 7007. Schlegel, H. B.; Sosa, C. *Chem. Phys. Lett*. **1988**, *145*, 329.

(37) Schlegel, H. B. *J. Chem. Phys*. **1986**, *84*, 4530. Schlegel, H. B. *J. Phys. Chem*. **1988**, *92*, 3075. Knowles, P. J.; Handy, N. C. *J. Chem. Phys*. **1988**, *88*, 6991.

(38) Sosa, C.; Schlegel, H. B. *Int. J. Quantum. Chem*. **1986**, *29*, 1001.

(39) Gonzalez, C.; Schlegel, H. B. *J. Chem. Phys*. **1989**, *90*, 2154. Gonzalez, C.; Schlegel, H. B. *J. Phys. Chem*. **1990**, *94*, 5523.

(40) This value was used in ref 2. For a discussion, see: Wong, M. W. *Chem. Phys. Lett*., **1996**, *256*, 391.

(41) Frisch, M. J.; Trucks, G. W.; Schlegel, H. B.; Gill, P. M. W.; Johnson, B. G.; Robb, M. A.; Cheeseman, J. R.; Keith, T.; Petersson, G. A.; Montgomery, J. A.; Raghavachari, K.; Al-Laham, M. A.; Zakrzewski, V. G.; Ortiz, J. V.; Foresman, J. B.; Peng, C. Y.; Ayala, P. Y.; Chen, W.; Wong, M. W.; Andres, J. L.; Replogle, E. S.; Gomperts, R.; Martin, R. L.; Fox, D. J.; Binkley, J. S.; Defrees, D. J.; Baker, J.; Stewart, J. P.; Head-Gordon, M.; Gonzalez, C.; Pople, J. A. GAUSSIAN 94, Revision B.3, Gaussian, Inc., Pittsburgh, PA, 1995.

(42) MOLCAS Version 4. Andersson, K.; Blomberg, M. R. A.; Fülscher, M. P.; Karlström, G.; Lindh, R.; Malmqvist, P.-Å.; Neogrády, P.; Olsen, J.; Roos, B. O.; Sadlej, A. J.; Schütz, M.; Seijo, L.; Serrano-Andrés, L.; Siegbahn, P. E. M.; Widmark, P. O. Lund University, Sweden, 1997.

(43) Gillies, C. W.; Kuczkowski, R. L. *J. Am. Chem. Soc.* **1972**, *94*, 6337.

(44) Selcuki, C.; Aviyente, V.; Aplincourt, P.; Ruiz- López, M. F., submitted.

(45) Lossing, F. P.; Tickner, A. W. *J. Chem. Phys.* **1952**, *20*, 907.

(46) Rebbert, R. E.; Laidler, K. J. *J. Chem. Phys.* **1952**, *20*, 574.

(47) Wu, G.; Shlykov, S.; Van Alsenoy, C.; Geise, H. J.; Sluyts, E.; Van der Veken, B. J. *J. Phys. Chem*. **1995**, *99*, 8589.

(48) Noe, E. A.; Raban, M. *J. Chem. Soc., Chem. Commun.* **1974**, 479.

(49) Herzberg, G. *Spectra of Diatomic Molecules*; Van Nostrand: New York, 1950. See also, for a theoretical computation: Vincent, M. A.; Hillier, I. H. *J. Phys. Chem.* **1995**, *99*, 3109.